Available online at www.sciencedirect.com

SCIENCE DIRECT®

Earth and Planetary Science Letters 223 (2004) 99–111

EPSL

www.elsevier.com/locate/epsl

Isotopic constraints on the cooling of the continental lithosphere

R.-M. Bedini, J. Blichert-Toft, M. Boyet, F. Albarède*

Ecole Normale Supérieure de Lyon, 69007 Lyons, France

Received 22 October 2003; received in revised form 1 April 2004; accepted 9 April 2004

Abstract

A new model of continuous diffusion of radiogenic isotopes was applied to mineral $^{147}Sm-^{143}Nd$ and $^{176}Lu-^{176}Hf$ data on low-temperature garnet-peridotite xenoliths from Cretaceous South African kimberlites. The radiometric ages are younger than the Archean whole-rock Re–Os and U–Pb ages and reflect that both the Sm–Nd and Lu–Hf chronometric systems remained open under the thermal conditions of the lithospheric mantle. The radiogenic character of Hf in garnets, however, indicates that even if essentially no pyroxene remained immune to the effects of metasomatic events, the core of many garnets may preserve memory of the long history of this mineral in the subcontinental lithosphere. The cooling rates deduced from the garnet Sm–Nd ages in the South African lithosphere are fairly low (40–105 °C Gy^{-1}), but compare well with values obtained on similar samples from different regions. These unexpectedly low values imply that the heat flow at the base of the subcontinental lithospheric mantle has changed only very slowly through time. They further support the recent suggestion that, as a result of viscous dissipation by plate bending, convection vigor and heat flow are to some extent decoupled, which argues against a thermal feedback on geodynamics. Modern convection may still be mining fossil heat stored in the lower mantle.

Keywords: cooling; lithosphere; garnet peridotite; Sm–Nd and Lu–Hf; closure temperature

1. Introduction

The Earth cools because it looses primordial heat and because the heat-producing isotopes of U, Th, and K decay through time. Understanding the Earth's cooling history revolves around the issue of the contribution of fossil heat to the modern surface heat flow. Observational constraints on this problem are scant and essentially qualitative. The standard interpretation of komatiites calls for the convective mantle to be somewhat hotter in the Archean than today, whereas the prevalence of old cratons as the major source of diamonds points to the Archean lithosphere being not much thinner than its modern equivalent. Here, we attempt a different approach, which is to assess the cooling rate of continents through isotopic methods. Because U, Th, and K are concentrated next to the surface of continents, the thermochronology of crustal rocks is dominated by the decay of radioactive heat sources. Although this problem does not arise in the deep lithosphere, temperature there is elevated enough that the chronometers never close entirely, and a new model on radiogenic ingrowth and volume diffusion therefore must be used [1]. Here we present new $^{147}Sm-^{143}Nd$

* Corresponding author. Tel.: +33-472-72-8414; fax: +33-472-72-8677.

E-mail address: albarede@ens-lyon.fr (F. Albarède).

0012-821X/$ - see front matter © 2004 Elsevier B.V. All rights reserved.
doi:10.1016/j.epsl.2004.04.012

and $^{176}Lu-^{176}Hf$ data on low-temperature garnet-peridotite xenoliths from Cretaceous South African kimberlites in order to estimate their cooling history. The Re–Os depletion ages of the peridotite xenoliths from the South African craton fall between 2.7 and 3.7 Ga [2,3], while U–Pb ages up to 2.7 Ga have been obtained on zircons of lower crustal xenoliths from the same localities [4,5].

Diffusion, as viscosity, is a thermally activated process. The age patterns registered by chronometric systems, such as $^{147}Sm-^{143}Nd$ and $^{176}Lu-^{176}Hf$, in minerals under high-temperature conditions may therefore be considered as a record of their thermal history. Radioactive decay produces radiogenic nuclides in excess of the abundance the host mineral would otherwise have in the absence of the parent nuclide. This excess is present whether or not the host mineral is at thermodynamic equilibrium with the surrounding mineral assemblage. Upon rapid cooling, as is the case for the continental crust, volume diffusion becomes less efficient and ceases over a relatively narrow temperature interval around a temperature known as the closure temperature [6]. Above their closure temperature, however, chronometric systems are leaky enough to be effectively unreliable for dating purposes, but still retentive enough to accumulate some amount of the radiogenic isotopes produced by in situ radioactive decay (Fig. 1). Consequently, these systems carry valuable information about the cooling history of the rock. In order to retrieve the cooling history of samples from the South African lithospheric mantle, we applied the analytical solution to the diffusion equation with variable temperature and radiogenic ingrowth [1] to $^{147}Sm-^{143}Nd$ and $^{176}Lu-^{176}Hf$ garnet ages in low-temperature peridotite xenoliths from South African kimberlites. We argue below that even if essentially no pyroxene were immune to the effects of metasomatic events, the core of many garnets may still preserve some memory of the long history of this mineral in the subcontinental lithosphere. Although this point is controversial [7], we contend that isotopic evidence for a protracted cooling history is preserved in garnet from lithospheric xenoliths.

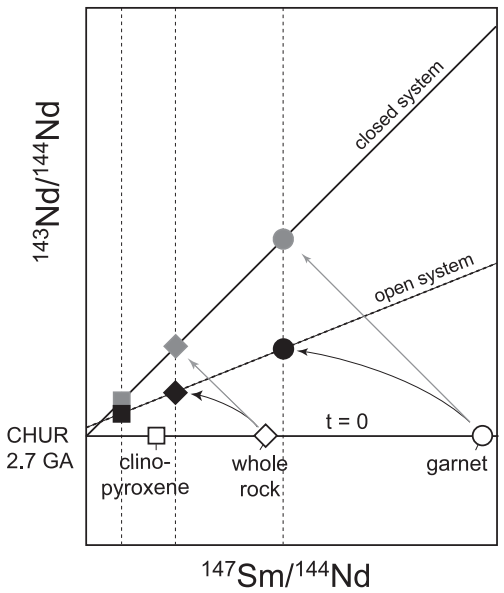

Fig. 1. Open-system evolution of a bi-mineralic (clinopyroxene-garnet) sample loosing part of its radiogenic ^{143}Nd to the interstitial medium. The decay of ^{147}Sm is exaggerated for illustration purpose. The reference closed-system isochron is represented with light-shaded symbols. The rock is supposed to have crystallized at 2.7 Ga with a chondritic (CHUR) isotope composition of Nd. Loss of ^{144}Nd and ^{147}Sm is neglected so that the abscissa of each mineral remains unaffected by diffusion loss. The perturbed whole-rock still defines an open-system 'isochron' with respect to the two minerals, but the slope does not reflect the age, and the intercept is no longer simply related to the initial isotopic composition of Nd. For a rock with more than two mineral phases, the minerals and the whole-rock do not form an alignment.

2. Analytical procedures

One hundred- to two hundred-milligram-sized garnet and clinopyroxene fractions were hand-picked from substantially larger mineral fractions that had been previously roughly separated using a Frantz magnetic mineral separator. Inclusion-bearing grains and minerals showing surface elements and fractures were meticulously avoided during the hand-picking. The overall relatively low concentrations measured for all mineral separates indicate that the attempted exclusion of both rare-earth-element (REE)- and Hf-bearing inclusions was successful. In order to minimize blank levels, the hand-picked minerals were not subjected to further unnecessary crushing, but dissolved whole. Prior to dissolution, the mineral grains were acid leached in an ultrasonic bath using both HF and HCl to eliminate any grain coatings

deposited either directly by crystallization of the kimberlite or by later alteration. Whole-rock powders likewise were acid leached to remove any secondary phases.

For isotope analyses, the mineral separates and whole-rock powders were attacked in steel-jacketed Teflon bombs for 1 week at 160 °C with mixed $^{149}Sm-^{150}Nd$ and $^{176}Lu-^{180}Hf$ spikes added to the samples from the outset of the dissolution procedure. Upon complete sample-spike homogenization, a Hf-bearing fraction was separated from a REE-bearing fraction on a cation-exchange column. Nd, Sm, and a combined Yb–Lu fraction were subsequently isolated from the latter on an HDEHP column, while Hf was further purified, first through an anion-exchange column so as to remove remaining matrix elements, then through a cation-exchange column serving to separate Ti and some Zr from the Hf [8–10]. Due to especially the low Hf concentrations of many of the samples, only double-distilled reagents and new resins were used throughout the dissolution and elution procedures. Total procedural Nd, Sm, Lu, and Hf blanks were <200, <20, <20, and <25 pg, respectively, which are all sufficiently low for even the most depleted of the samples to be blank-insensitive.

The isotopic analyses of Nd, Sm, Hf, and Lu were carried out by MC-ICP-MS on the VG Plasma 54 instrument in Lyon following the procedures described in detail in [8,10]. In order to monitor machine performance, the La Jolla Nd and JMC-475 Hf standards were run systematically before and after each sample and gave, throughout this study, 0.511858 ± 0.000018 for $^{143}Nd/^{144}Nd$ and 0.282160 ± 0.000010 for $^{176}Hf/^{177}Hf$ (two standard deviations), corresponding to an external reproducibility of 35 ppm for both isotope systems.

3. Results

In this study, low-temperature peridotites were preferred to high-temperature peridotites because minerals in the latter may not be able to preserve measurable isotopic disequilibrium. With one exception, Louwrencia sample JJG2513 from Gibeon, the Cretaceous (ca. 90 Ma old) kimberlite pipes investigated here all erupted on the Archean craton. Nine xenoliths were selected because of their apparent lack of metasomatic alteration, as well as using the criterion that their temperatures and pressures lie near the standard continental geotherm (Fig. 2), thereby minimizing the effects of possible metasomatic disturbances. Temperatures and pressures were estimated from electron probe data on pyroxenes and garnets using mineral equilibrium thermometers and barometers (Table 1). Pressures of 3.1–4.1 GPa and temperatures of 770–1100 °C define a geotherm which is in agreement with heat flow values [11,12]. The isotopic data are reported in Table 2. The distribution of Sm–Nd ages in South African garnet-peridotite xenoliths is reminiscent of the corresponding ages of eclogite inclusions in kimberlites from other localities: the South African craton [2], Siberia [13–15], Montana [16]. The combined Sm–Nd and Lu–Hf isotope systematics of these rocks further resemble those of the garnet-peridotite inclusions from the Somerset Island kimberlites in the Canadian Arctic [17,18].

The covariation of Nd and Hf isotopic compositions of clinopyroxene and garnet is shown in Fig. 3. The extent of the isotopic decoupling between these two elements stands in stark contrast to the observation of extremely well-correlated isotopic compositions of Hf and Nd in most oceanic basalts (e.g. [19]). Unusually radiogenic Hf is observed in clinopyroxene in association with isotopically less distinctive Nd, which is reminiscent of clinopyroxene data on Ha-

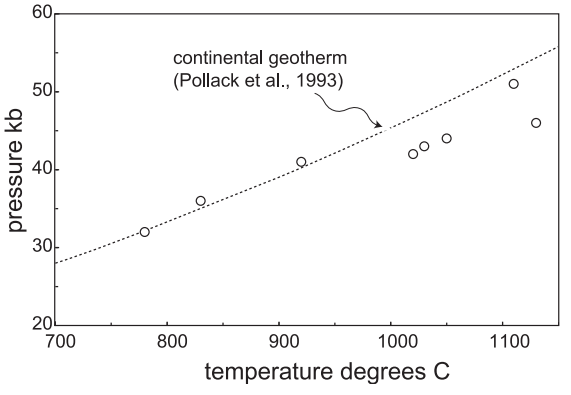

Fig. 2. Temperature and pressure of the nine samples from the South African craton studied in the present work. The agreement with data from [12] is a strong indication that the samples were not severely perturbed by late-stage volcanic metasomatic events.

Table 1
Temperature and pressure estimates deduced from various geo-thermo-meters and geo-baro-meters

Sample	T opx–cpx	P opx–gt	T ga–cpx	T ga–cpx	T_0 (°C)	$-dT/dt$ (°C Gy^{-1})		
	(°C) (1)	(GPa) (2)	(°C) (3)	(°C) (4)	a=1 cm	a=1 cm	a=1 mm	a=1 mm
Age of the lithosphere (Ga)					2.7	2.7	2.7	4.0
Jagersfontein								
KBJ15	780 ± 30	3.1 ± 2	740 ± 20	760 ± 20	884 ± 15	n.d.	3 ± 15	6 ± 11
KBJ18	770 ± 30	3.2 ± 2	n.d.	780 ± 10	894 ± 5	n.d.	n.d.	n.d. ± 0
Finsch								
FRB1514	1100 ± 40	5.1 ± 2	1110 ± 10	n.d.	1247 ± 8	62 ± 8	63 ± 8	52 ± 7
Bultfontein (Kimberley)								
BD2356	850 ± 25	3.6 ± 1	n.d.	830 ± 10	888 ± 5	n.d.	20 ± 5	16 ± 3
BD2393	1050 ± 40	4.6 ± 2	1130 ± 20	n.d.	1146 ± 5	39 ± 6	41 ± 5	30 ± 4
Liqhobong (N. Lhesoto)								
LLQ3	1070 ± 55	4.4 ± 2	1100 ± 10	1050 ± 10	1305 ± 14	104 ± 15	104 ± 14	82 ± 12
LLQ5	1040 ± 35	4.3 ± 2	1050 ± 10	1030 ± 10	1152 ± 6	46 ± 7	48 ± 6	38 ± 5
LLQ7	1045 ± 50	4.2 ± 3	1070 ± 10	1020 ± 20	1190 ± 8	61 ± 9	63 ± 8	48 ± 6
Louwrencia (Gibeon) (5)								
JJG2513	960 ± 20	4.1 ± 1	n.d.	920 ± 20	1129 ± 11	73 ± 19	82 ± 11	56 ± 7

Cooling rates inferred from the Sm–Nd isotopic data on garnet.
(1) Average of three geo-thermometers [55–57]; (2) [58]; (3) [59], temperatures consistent with values deduced from [60,61]; (4) [62]. n.d. = values outside the range of validity. (5) Off-craton sample. All other samples are on-craton. A first estimate of temperatures by a two-pyroxene thermometer [55–57] allows pressure to be estimated from the temperature-dependent garnet–clinopyroxene geo-barometer [58]. The temperatures back-calculated from the garnet–clinopyroxene couples [59–61] are consistent with the temperature deduced from the pyroxene pairs. Errors are one standard deviation. The cooling rates are estimated from the relationship [1] between time and the age 'deficit' (Fig. 1) and from the two-pyroxene temperatures assumed to record modern lithospheric conditions. Errors are propagated from uncertainties in [32].

waiian peridotites [20]. Hf is isotopically even more extreme in garnets.

4. Discussion

Four key observations are made.

(1) The general lack of alignment of minerals with their corresponding whole-rocks on Lu–Hf and Sm–Nd isochrons requires the presence of additional mineral carriers of Nd and Hf, presumably some minute, easily perturbed mineral phases, such as apatite and other types of phosphate [21,22].
(2) Some Sm–Nd clinopyroxene-garnet ages are negative. This is normally interpreted [23,24] as indicating that, in clinopyroxene, the Sm–Nd system, and possibly all other chronometric systems as well, has been reset upon reaction of the rock with fluids and magmas, or even upon

Notes to Table 2:
Ages are obtained from the two-point clinopyroxene-garnet isochrons. Garnet model ages are with respect to a 2.7-Ga-old lithosphere with chondritic uniform reservoir (CHUR) properties.
gt = garnet; cpx = clinopyroxene; wr = whole-rock.
[a] Sm, Nd, Lu, and Hf isotopic compositions and concentrations measured by MC-ICP-MS (VG Plasma 54). [Sm], [Nd], [Lu], and [Hf] and $^{147}Sm/^{144}Nd$ and $^{176}Lu/^{177}Hf < 0.3\%$ (2σ errors). Sm, Nd, Lu, and Hf concentrations determined by isotope dilution.
[b] Uncertainties reported on Nd and Hf measured isotope ratios are $2\sigma\sqrt{n}$ analytical errors in last decimal place, where n is the number of measured isotopic ratios. $^{143}Nd/^{144}Nd$ and $^{176}Hf/^{177}Hf$ normalized for mass fractionation to, respectively, $^{146}Nd/^{144}Nd = 0.7219$ and $^{179}Hf/^{177}Hf = 0.7325$. CHUR parameters (today): $^{143}Nd/^{144}Nd = 0.512638$, $^{147}Sm/^{144}Nd = 0.1967$, $^{176}Hf/^{177}Hf = 0.282772$, $^{176}Lu/^{177}Hf = 0.0332$. The very high CHUR Lu–Hf model ages of the LLQ3 and LLQ5 garnets are a result of their particularly low Lu/Hf ratios.

Table 2
$^{147}Sm-^{143}Nd$ and $^{176}Lu-^{176}Hf$ whole-rock and mineral isotope and concentration data for low-temperature garnet-peridotite xenoliths from Cretaceous South African kimberlites

Sample		[Sm][a] (ppm)	[Nd][a] (ppm)	($^{147}Sm/^{144}Nd$)[a]	($^{143}Nd/^{144}Nd$)[b] $\pm 2\sigma\sqrt{n}$	[Lu][a] (ppm)	[Hf][a] (ppm)	($^{176}Lu/^{177}Hf$)[a]	($^{176}Hf/^{177}Hf$)[b] $\pm 2\sigma\sqrt{n}$	cpx–ga age (Ma)		ga model age (Ma) 2.7 Ga CHUR	
										Sm–Nd $\pm 2\sigma$	Lu–Hf $\pm 2\sigma$	Sm–Nd $\pm 2\sigma$	Lu–Hf $\pm 2\sigma$
Jagersfontein													
KBJ15	gt	1.644	2.743	0.362	0.512701 ± 29	0.3437	0.0715	0.6821	0.296055 ± 18	349 ± 9	859 ± 3	1283	1130
	cpx	6.38	54.44	0.07088	0.512036 ± 7	0.01819	0.4891	0.00528	0.284744 ± 9				
	wr	1.566	13.26	0.07137	0.512424 ± 5	0.02115	0.103	0.02916	0.283786 ± 17				
KBJ18	gt	1.49	1.202	0.7503	0.513398 ± 13	0.4553	0.1322	0.4889	0.288918 ± 16	326 ± 3	560 ± 3	763	833
	cpx	5.82	30.15	0.1167	0.512044 ± 6	0.00628	0.8135	0.00109	0.283619 ± 12				
	wr	0.8396	4.712	0.1077	0.512587 ± 4	0.03724	0.3101	0.01704	0.283034 ± 6				
Finsch													
FRB1514	gt	1.041	2.502	0.251	0.512032 ± 11	0.2427	0.7856	0.04385	0.283155 ± 4	102 ± 11	191 ± 21	1414	2490
	cpx	1.267	11.64	0.06580	0.511908 ± 8	0.003	0.4002	0.00106	0.282997 ± 14				
	wr	0.2439	1.466	0.1006	0.512084 ± 12	0.02019	0.1821	0.01573	0.282714 ± 10				
Bultfontein (Kimberley)													
BD2356	gt	0.613	1.094	0.3387	0.512110 ± 7	0.4020	0.1685	0.3386	0.290995 ± 20	99 ± 7	1219 ± 5	1108	1508
	cpx	3.585	28.63	0.07568	0.511939 ± 4	0.00894	1.714	0.00074	0.282950 ± 6				
	wr	0.9569	6.802	0.08506	0.512301 ± 5	0.06078	0.3156	0.02733	0.283324 ± 19				
BD2393	gt	1.186	2.242	0.3196	0.512363 ± 5	0.3277	0.6914	0.06727	0.283150 ± 10	− 14 ± 8	157 ± 21	1294	1633
	cpx	3.344	22.65	0.08926	0.512384 ± 8	0.01142	1.393	0.00116	0.282949 ± 25				
	wr	0.9823	5.945	0.09989	0.512513 ± 4	0.03426	0.4627	0.01051	0.282972 ± 22				
Liqhobong (N. Lhesoto)													
LLQ3	gt	1.503	3.819	0.238	0.512350 ± 13	0.05503	0.5031	0.01553	0.282904 ± 8	− 923 ± 23	474 ± 48	1727	>4500
	cpx	4.404	16.68	0.1597	0.512821 ± 6	0.0123	5.899	0.0003	0.282764 ± 6				
	wr	0.2074	1.079	0.1162	0.512719 ± 10	0.00451	0.1433	0.00447	0.282941 ± 80				
LLQ5	gt	1.502	3.384	0.2683	0.512336 ± 7	0.04031	0.5087	0.01125	0.283113 ± 8	− 631 ± 17	1503 ± 66	1370	>4500
	cpx	3.751	15.02	0.151	0.512819 ± 12	0.00594	2.494	0.00034	0.282792 ± 6				
	wr	0.3836	2.077	0.1117	0.512759 ± 6	0.00512	0.1754	0.00414	0.282845 ± 17				
LLQ7	gt	0.5042	1.111	0.274	0.512115 ± 11	0.205	0.2449	0.1188	0.285742 ± 8	− 825 ± 17	1252 ± 7	1525	2029
	cpx	4.107	16.17	0.154	0.512761 ± 8	0.01752	3.201	0.00078	0.282855 ± 5				
	wr	0.3164	1.541	0.1241	0.512722 ± 10	0.00731	0.2164	0.00479	0.282884 ± 6				
Louwrencia (Gibeon)													
JJG2513	gt	0.05574	0.1291	0.2611	0.512624 ± 27	0.1772	0.0075	3.354	0.353456 ± 153	− 91 ± 15	1076 ± 4	1734	1108
	cpx	2.26	14.15	0.09637	0.512722 ± 6	0.00605	0.7544	0.00114	0.283075 ± 12				
	wr	0.2762	1.774	0.09408	0.512775 ± 10	0.01373	0.1019	0.01913	0.283343 ± 15				

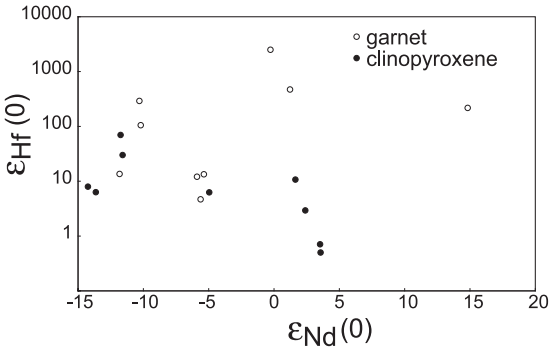

Fig. 3. Present-day Nd and Hf isotope compositions of clinopyroxenes and garnets in xenoliths from the South African craton (in epsilon or parts per 10 000 notation.) Note the log-scale for Hf. The strong decoupling between the two systems suggests that Hf is far more resistant to diffusional loss and metasomatism than Nd.

introduction of clinopyroxene into the peridotite during metasomatic events. The elemental and isotopic patterns of this mineral are thought to be perturbed by the metasomatism accompanying kimberlite eruption. The ages indicated by clinopyroxene-garnet mineral isochrons are therefore often useless for any practical purposes [25].

(3) The Hf isotope compositions of some of the garnets (e.g., BD2356, KBJ15, or JJG2513) are extremely radiogenic, indicating that these garnets are definitely ancient.

(4) The two-point Lu–Hf garnet–clinopyroxene ages are generally older than the corresponding Sm–Nd ages and never negative, which suggests that radiogenic Hf diffuses out of garnet more slowly than does radiogenic Nd [26]. The decoupling of Hf and Nd isotope compositions in garnet, and to a lesser extent in clinopyroxene, may be relevant to the occasional decoupling observed between these two isotope systems in oceanic basalts (e.g. [19]).

To a certain extent, garnet is also affected by metasomatic processes [25,27], but laser ablation and ion probe analyses have demonstrated these effects to be limited to the outer ca. 100-μm rim around the crystals [28,29], a part which is largely eliminated during mineral separation and ensuing acid leaching. We therefore turned to model ages and used a 2.7-Ga-old chondritic uniform reservoir model (CHUR) as the reference for initial Nd and Hf isotope compositions to calculate these ages. In all cases but two (the Lu/Hf ratios of LLQ3 and LLG5), the parent/daughter ratios of garnet are high enough for the CHUR model ages of these minerals to be rather insensitive to the initial Nd and Hf isotope compositions assumed for the system.

Provided garnet crystallized over a short period of time, i.e., that a crystallization age can be defined, this age has to be younger than the age of the xenoliths themselves and older than the oldest ages indicated by the CHUR garnet model ages. Metasomatic perturbations have to some extent affected the Sm–Nd and Lu–Hf systematics of garnet, but, for the following reason, this is probably not critical to the present interpretation. Let us consider as an example that Nd consists of two components, the purely radiogenic ^{143}Nd, which has accumulated since garnet formation without being lost to the ambient rock, and common unradiogenic Nd. If metasomatism perturbs one component, it perturbs the other as well. In other words, injecting kimberlitic liquid with an ε_{Nd} in the range of −10 to +2 [30] into the fractures of an old garnet, so that a substantial fraction of the Nd in the mineral is replaced by Nd from the kimberlite and the garnet Sm/Nd ratios modified, will not leave enough radiogenic Nd for the Sm–Nd system in the garnet to record an old age. This effect is greatly amplified by the fact that self-diffusion is much faster than chemical diffusion (e.g., [31,32]). If the Sm/Nd ratio is substantially perturbed, very little radiogenic Nd should be preserved in garnets today to record an old age. The case for Hf is identical. The 1.0–1.5 Ga Lu–Hf ages of four clinopyroxene-garnet pairs and CHUR model ages of up to 2.5 Ga (Table 2) do not support an overall recent crystallization or recrystallization of garnet [28] or even recent extensive equilibration with metasomatic fluids. Although the existence of metasomatic perturbations cannot be discounted, they seem largely restricted to the outer rim of the garnets, leaving the core reasonably pristine. In addition, the model ages are distinct for both the Sm–Nd and Lu–Hf systems: short of strong independent evidence, these ages therefore cannot be considered as dating identifiable metasomatic events taking place within the subcontinental lithosphere.

The very existence of fairly radiogenic Nd and Hf in most garnets therefore requires that these crystals have been in existence for billions of years and are not

simply a product of recent metasomatism. This is consistent with available whole-rock $^{187}Re-^{187}Os$ data [15,33], which indicate that the protolith formed at the end of the Archean. We stress that, since the temperatures recorded by the mineral assemblages exceed any acceptable blocking temperature (≈ 800 °C for REE and slow cooling, see below), mineral ages should not be referred to as closure ages. The tenet that the geochemical evolution of deep peridotites is punctuated by metasomatic events separated by long periods of chemical equilibrium frozen below the blocking temperature of exchange reactions between minerals does not hold in the lithosphere where temperatures well in excess of 800°C constantly prevail (Fig. 4). Temperature estimates derived from mineral compositions are commonly only slightly higher than that of the average continental geotherm at the same depth. This confirms that most of the cooling history of the host xenoliths took place above the blocking temperature (≈ 750 °C) of the thermometers themselves [34] and, in general, above the blocking temperature of most mineral reactions. Consequently, the geochemical characteristics of chemical and isotopic equilibrium prevailing during garnet formation are unlikely to have been preserved to the present day and thus the modern mineralogy of ultramafic xenoliths (e.g., [25]) does not truly constrain the nature of their protolith nor the history of their constituent minerals. A vivid illustration of this difficulty is that, regardless of the intensity of metasomatic alteration, garnet and clinopyroxene are neither isotopically (this work and many previous isotopic studies) nor chemically equilibrated [28]. The isotope compositions of Nd and Hf in garnet rather reflect the state of an actively open system serendipitousy captured at the time of kimberlite eruption.

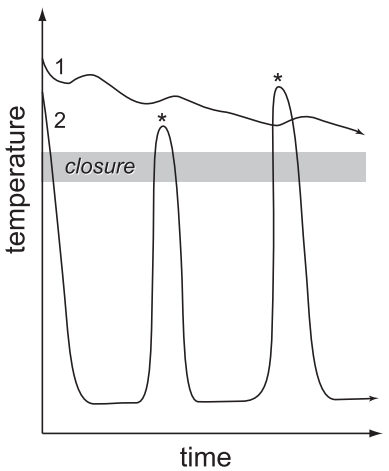

Fig. 4. Two contrasting models representing the thermal evolution of a mineral hosting a chronometer. (1) Open system in a slowly cooling lithosphere (Eq. (3) applies). (2) Closed system evolution punctuated by thermal (metasomatic) events (*). For the Sm–Nd chronometer, the closure temperature is ≈ 750 °C. The actual situation in the subcontinental lithospheric mantle is best described by model 1.

The model used here to interpret the data assumes that garnet formed with its observed grain size during a geologically speaking short episode and kept leaking its excess radiogenic nuclides to its surroundings through intergranular exchange. Most notably, the excess radiogenic Nd and Hf ingrowth, which is particularly large with respect to any neighboring phase, inclusive of injected melts and liquids, is continuously lost to the ambient medium. We assume radial volume diffusion through a spherical mineral with zero concentration at the surface [1]. To where the radiogenic Nd and Hf lost by garnet eventually go, probably into minute grains of accessory minerals such as apatite [21,22] in which they become diluted by common unradiogenic Nd and Hf, is immaterial to the present discussion. The intergranular medium characterized by lattice mismatch and abundant impurities represents a fast path of diffusion (e.g., [35]) and the effect of accessory phases present in this medium can be neglected. Although Ca, Al, Ti, and other elements have been observed to segregate between crystals, the lack of observable interfaces as well as compositional variability and unit cell-like thickness of such boundaries (1–5 nm) [36] do not qualify grain boundaries as true mineral phases. Regardless of their enrichment with respect to adjacent crystals, the minuscule volume of these boundaries does not allow them to host a substantial fraction of the radiogenic isotope inventory. Grain boundaries cannot therefore buffer isotopically the major minerals even for incompatible elements, which is in agreement with the first-order interpretation of isotopic disequilibrium in xenoliths. As long as a mineral hosting a parent–daughter system remains at high temperature, the excess of the radiogenic isotope is continuously lost by volume diffusion to the intergranular medium

from where it migrates into other mineral phases or is transported out of the rock by circulating fluids and melts.

The equations for simultaneous accumulation of radiogenic isotopes and loss by volume diffusion in a spherical mineral held above the closure temperature have been solved [1] for the case where the reciprocal of absolute temperature T varies linearly with time t, i.e., under the conditions used to define the closure temperature itself [6], and with the cooling rate parameter α defined as $\mathrm{d}T^{-1}/\mathrm{d}t$. In a spherical mineral with radius a, the diffusion coefficient $\mathscr{D}_D$ of the radiogenic (daughter) isotope under consideration follows the Arrhenius law

$$\mathscr{D}_D(t) = \mathscr{D}_D^{\dagger}\exp\left(-\frac{E_D}{RT[t]}\right) \quad (1)$$

in which R is the gas constant, E_D the activation energy, and $\mathscr{D}_D^{\dagger}$ the pre-exponential factor. The parent nuclide is assumed to be homogeneously distributed within the crystal. Conservation of the number of parent and daughter nuclides requires that:

$$\frac{\partial}{\partial t}(P+D^*) = \mathscr{D}_D(t)\left(\frac{\partial^2 D^*}{\partial r^2}+\frac{2}{r}\frac{\partial D^*}{\partial r}\right)$$

$$= \mathscr{D}_D(t)\left[\frac{\partial^2 (P+D^*)}{\partial r^2}+\frac{2}{r}\frac{\partial (P+D^*)}{\partial r}\right] \quad (2)$$

where the asterisk denotes the radiogenic nuclide and r $(0<r\leq a)$ is the radial coordinate. Because it is conserved in a closed system, the sum $P+D^*$ makes a convenient variable for the model. The age 'deficit' ΔT at time t is [1]:

$$\Delta T \approx \frac{a^2}{\mathscr{D}_D^{\dagger}} e^{E_D/RT_0}\left(\tau-\frac{1}{15}+6\sum_{n=1}^{\infty}\frac{e^{-n^2\pi^2\tau}}{n^4\pi^4}\right) \quad (3)$$

where T_0 is the temperature at $t=0$ and

$$\tau = \int_0^t \frac{\mathscr{D}_D(t')}{a^2}\mathrm{d}t' = \frac{R}{E_D}\frac{\mathscr{D}_D^{\dagger}}{\alpha a^2}e^{-E_D/RT_0}\left(1-e^{-E_D\alpha t/R}\right) \quad (4)$$

For a radiogenic isotope with known diffusive properties, each mineral of known age t and with an age deficit ΔT therefore gives a relationship between the cooling rate and T_0. An important property is that the dependence of the cooling rate parameter α on T_0, a, and t is weak, which makes α estimates through this method relatively robust.

The diffusive properties of Hf, or any other high-field strength element, still remain to be determined. In the absence of such data, we instead use existing data for Sm chemical diffusion [32] as a proxy for Nd. Self-diffusion, notably exchange of isotopes, is known to be faster than chemical diffusion by an order of magnitude or more (e.g., [31]), but the last equation shows that the uncertainty on $\mathscr{D}_D^{\dagger}$ is simply embedded in that on the grain size a. We report in Fig. 5 the relationship between the cooling rate $-\alpha T^2$ and T_0 for two mineral grain sizes ($a=0.1$ and 1 cm). Using different mantle compositions, such as for example the depleted mantle, or different reservoir ages instead of CHUR, does not affect the results substantially. The error bars on the diffusion parameters [32] were propagated and found to affect the results by at most 20%. Using the temperatures inferred from the two-pyroxene geothermometer, back-calculated to the time of crystallization is occasionally inconsistent with the calculated cooling rate $-T_0$ trajectories, in particular when the blocking temperature is approached (e.g., KBJ15 and KBJ18). However, regardless of the assumptions made on temperature, the cooling rates are well constrained, simply because when temperature is high enough, α depends on T_0 only very slightly (Fig. 5). Using the modern two-pyroxene temperatures of the present samples, we calculated a range of cooling rates between 40 and 105 K Gy^{-1} with a weighted average of 62 ± 11 K Gy^{-1} (Table 1). Changing the crystallization age from 2.0 to 4.0 Ga, the grain size from 0.1 to 1 cm, or using a pre-exponential factor an order of magnitude higher to account for faster self-diffusion, is virtually inconsequential to the cooling rate values obtained. In spite of the much older emplacement ages of the host kimberlites (1180 Ma) [2], similar garnet-peridotite inclusions from the Premier mine, Kimberley, provide cooling rates consistent with our results (Fig. 6).

Peridotite xenoliths from Cretaceous Somerset Island kimberlites, Canadian Arctic [37], give Os lithospheric residence ages of $\approx$ 2.6 Ga [38] (Fig. 6). With one exception, the Sm–Nd data for these rocks [17] yield slightly slower cooling rates (<40 °C Gy^{-1}). This range is consistent with the range of cooling

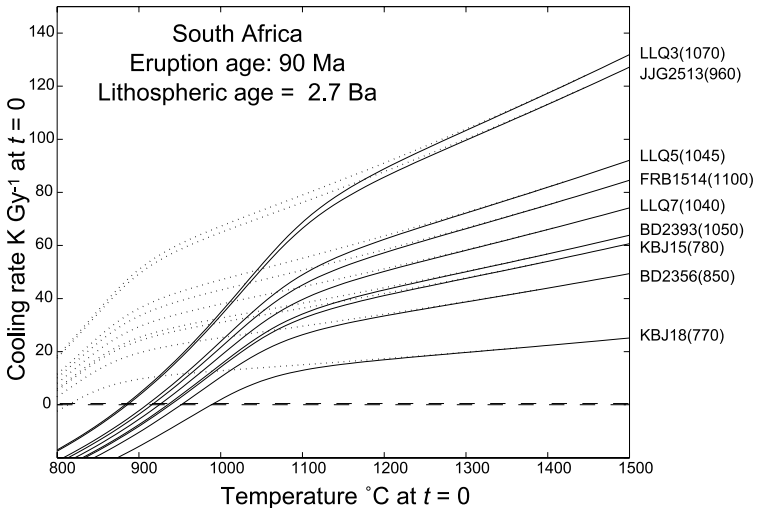

Fig. 5. Cooling rates of garnet-peridotite xenoliths from South Africa deduced from Sm–Nd isotopic data on garnets (Table 2) and the diffusive properties of Sm (used as a proxy for Nd) [32] in this mineral. The lines plotted represent the relationship between the cooling rate, calculated as $-\alpha T^2$ and time t for spherical minerals deduced from Eqs. (1) and (2) [1]. Solid and dotted lines are for radii of 1 cm and 1 mm, respectively. The sample numbers and the two-pyroxene temperature in °C of each sample are labelled on the right axis.

rates indicated by Nd isotope analyses of garnet peridotite [3] and eclogite [13,14] xenocrysts from the Paleozoic kimberlites of Yakutia (Fig. 6). Two garnet peridotites (H69-15F and W210) from the Tertiary Paleogene kimberlites of Williams, Montana [16], also reveal a similar cooling history (Fig. 6). Two other Montana samples, however, give a much faster cooling rate (>100 °C Gy^{-1}), which may reflect the rapid dissipation of a local thermal perturbation. Again, these estimates are fairly robust: changing the age of the lithosphere or the grain size has only little effect on the resulting cooling rates.

The cooling rate of the subcontinental lithosphere is only indirectly related to the cooling rate of the convective mantle. Because of the mid- to late-Archean age of the South African lithosphere, the amount of heat inherited from its formation, and still retained until today, is small. This can be simply demonstrated with an application of Kelvin's solution [39]:

$$T(z,t) = T(\infty)\mathrm{erf}\left(\frac{z}{2\sqrt{\kappa t}}\right) \quad (5)$$

After 3 Gy, the temperature in a semi-infinite hot medium of thermal diffusivity κ at a depth $z \approx 100$ km has declined to less than 20% of its initial value. The temperature of the subcontinental lithospheric mantle is therefore controlled by the heat flow from the underlying convective mantle, and the lithospheric levels feeding the kimberlite eruptions with xenoliths are thermally relaxed. As indicated above, the strong discordance between Nd and Hf garnet ages requires that post-Archean thermal pulses do not account for the current thermal state of the lithosphere. Assuming a steady-state distribution of radioactive heat sources $H(z)$ decreasing exponentially with depth z [40]:

$$T(z) = T_0 + \frac{q_l}{K}z + \theta(1 - e^{-z/a}) \quad (6)$$

where K stands for the thermal conductivity of the lithosphere, a for the depth-scale over which heat production is reduced by a factor e ($\approx$ 8 km), and q_l for the heat flow at the base z_l of the lithosphere (note $a \ll z_l$). Temperature θ is defined as

$$\theta = \frac{a^2 H(0)}{\kappa C_P} \quad (7)$$

in which C_P stands for the specific heat of the lithosphere. The radioactive heat sources decay with time as

$$\frac{dH(z)}{dt} = -\lambda^* H(z) \quad (8)$$

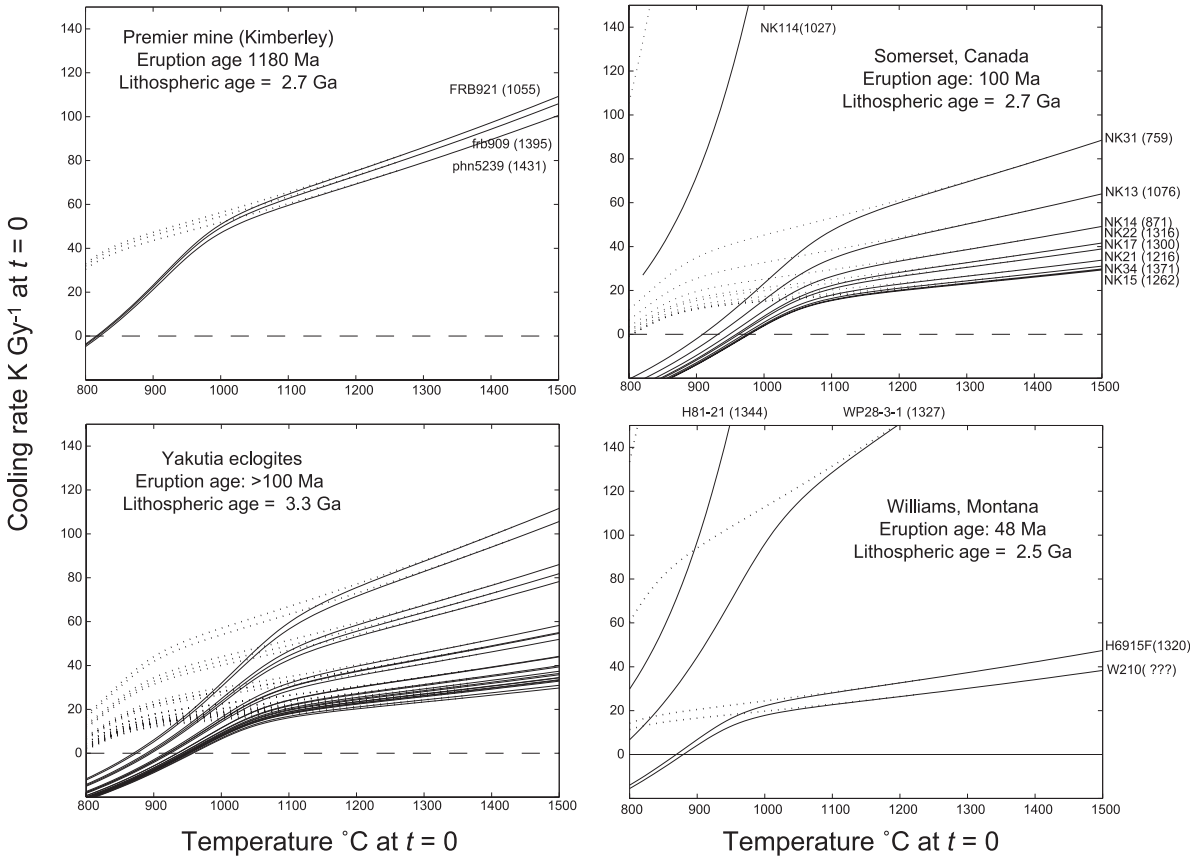

Fig. 6. Same as Fig. 4, but for garnet from peridotite xenoliths from other localities. Upper left: Premier mine, Kimberley [2]. Upper right: Somerset Island, Canadian Arctic [17]. Bottom right: Williams, Montana [16]. Bottom left: eclogites from Yakutia [13,14].

where λ^* is a decay constant compounded between those of the heat-producing radioactive nuclides [45]. A satisfactory approximation for q_1 therefore is:

$$q_1 \approx K\Delta T/z_1 \tag{9}$$

where $\Delta T = T(z_1) - T(0) - \theta$. The relative rate of change of mantle heat flow at depth $z_1 \gg a$ becomes:

$$\frac{1}{q_1}\frac{\mathrm{d}q_1}{\mathrm{d}t} \approx \frac{1}{\Delta T}\left[\frac{\mathrm{d}T(z_1)}{\mathrm{d}t} + \lambda^*\theta\right] \tag{10}$$

where λ^* is the compounded decay constant of the heat-producing elements, which varies within the range of 0.20–0.41 Gy^{-1} for post-Archean times. This expression reflects that the rate of lithospheric cooling combines the reduction of the heat flow from the convective mantle with the decay of crustal U, Th, and K. Depending on which crustal U, Th, and K contents are used [41,42], θ may vary from 50 to 100 K, and $\lambda^*\theta$ from 10 to 40 K Gy^{-1}, while $\Delta T \approx 700$–1000 K. One strong implication of this result is that although the cooling rate of the subcontinental lithosphere is already small, a large part (20–80%) of this cooling is still due to the radioactive decay of crustal heat sources. The heat flow at the base of the South African lithosphere has therefore varied only very little, on the order of a few percent per billion years, since the late Archean. The different cooling rates obtained for the South African and North Canadian cratons are likely to reflect different inventories of radioactive heat sources in their respective upper crusts.

Radioactive heat production has declined by a factor of two since the late Archean and part of the fossil heat inherited from the Earth's accretion has inevitably been lost. An empirical estimate suggests that the temperature in the convective mantle declined by 150 K Gy^{-1} over the last 3 billion years [43]. The gradual phasing out of komatiites as common lavas since the late Archean confirms this viewpoint. The inferred decline in mantle temperature contrasts with the rather steady heat flow deduced from the present study. The dominant paradigm of mantle convection of the last 30 years [44–46] regards mantle temperature as controlled by its feedback on convection through the temperature dependence of viscosity. It further predicts that the heat flow (Nusselt number *Nu*) from the mantle will change strongly with convective instability (Rayleigh number *Ra*):

$$Nu = \left(\frac{Ra}{Ra_{\mathrm{crit}}}\right)^{\beta} \tag{11}$$

where Ra_{crit} is the critical Rayleigh number at the onset of convection and β is a constant which, for feedback through the temperature dependence of viscosity, takes a value of ≈ 0.3 [47]. Combining this expression with the temperature-dependent viscosity and the radioactive decay of heat sources, results in a secular rate of mantle temperature T_{m} variation of:

$$\frac{\mathrm{d}T_{\mathrm{m}}^{-1}}{\mathrm{d}t} = \frac{\lambda^{*}R}{\beta E_{v}} \tag{12}$$

in which R stands for the gas constant and E_v for the creep activation energy ≈ 500 J mol^{-1}. This model predicts that mantle temperature decreases through time by ≈ 135 K Gy^{-1}. The well-known problem [46–48] with such a fast cooling rate is that unless a very substantial proportion of the heat-producing elements is concealed in the lower mantle, the modern Earth seems to be loosing far too much fossil heat with the implication that the Archean mantle must have been far hotter than commonly accepted based on geological evidence. The slow cooling rate inferred from the present work on kimberlite inclusions and from the chemistry of ancient basalts [43] for both the subcontinental lithosphere and the asthenosphere adds to the evidence that the mantle is not cooling as fast as implied by the thermal feedback theory.

Christensen [46] questioned such a thermal feedback through temperature-dependent viscosity, showing that the Archean thermal catastrophe could be avoided if $\beta \gg 0.3$. The stagnant-lid model of Davaille and Jaupart [49], in which strong temperature-dependent viscosity induces the formation of a thick rigid lithosphere resisting subduction, satisfies Christensen's criteria, but seems inconsistent with geological evidence of plate tectonics. Conrad and Hager [50] proposed a less extreme model, in which convection is essentially regulated by the bending of lithospheric plates at subduction zones. This results in efficient decoupling of surface heat flow and vigor of mantle convection, as β values are much smaller than 0.3. Korenaga [51] further observed that dehydration of the upper mantle upon melting contributes to the stiffening of the asthenosphere and thereby contributes to slowing down the pace of plate tectonics. Since in these dissipation-controlled models, the resistance of the lithosphere to bending and subduction helps sequester fossil radiogenic heat at depth, it also works against fast cooling of the mantle.

Only a few lithospheric plates reach the core–mantle boundary [52] and modern gardening of the deep mantle by only a small number of large, dense plates may not be very efficient at mining deep fossil heat. The modern imbalance between surface heat flow and radioactive production (low Urey number) may reflect that either heat was sequestered at depth by an early layering of the mantle [53] or the lower mantle remains only poorly stirred by the few sinking plates that have enough negative buoyancy to reach the core–mantle boundary [54].

Acknowledgements

This work benefited financially from the support of the Training and Mobility Program of the European Union and of Institut National des Sciences de l'Univers. The help of Philippe Télouk with the mass spectrometer and Jean-Louis Bodinier with the mineralogy is gratefully acknowledged. This work was partly completed while two of us (FA and JBT) were staying at Caltech. Discussions with Dave Stevenson, Take-

hiko Hiraga, and Dave Kohlstedt were particularly appreciated and thorough reviews by Rick Carlson, Bill Griffin, and Graham Pearson helped us crystallize some of the key arguments. ***[SK]***

References

[1] F. Albarède, The thermal history of leaky chronometers above their closure temperature, Geophys. Res. Lett. 30 (2003) DOI: 10.1029/2002GL016484.

[2] D.G. Pearson, R.W. Carlson, S.B. Shirey, R.R. Boyd, P.H. Nixon, Stabilization of Archean lithospheric mantle: a Re–Os isotope study of peridotite xenoliths from the Kapvaal craton, Earth Planet. Sci. Lett. 134 (1995) 341–357.

[3] D.G. Pearson, S.B. Shirey, R.W. Carlson, R.R. Boyd, N.P. Poknlenko, N. Shimizu, Re–Os, Sm–Nd, and Rb–Sr isotope evidence for thick Archean lithospheric mantle beneath the Siberian craton modified by metasomatism, Geochim. Cosmochim. Acta 59 (1995) 959–977.

[4] J.B. Dawson, S.L. Harley, R.L. Rudnick, T.R. Ireland, Equilibration and reaction in Archaean quartz-sapphirine granulite xenoliths from the Lace kimberlite pipe, South Africa, J. Metamorph. Geol. 15 (1997) 253–266.

[5] M.D. Schmitz, S.A. Bowring, Constraints on the thermal evolution of continental lithosphere from U–Pb accessory mineral thermochronometry of lower crustal xenoliths, southern Africa, Contrib. Mineral. Petrol. 144 (2003) 592–618.

[6] M.H. Dodson, Closure temperature in cooling geochronological and petrological systems, Contrib. Mineral. Petrol. 40 (1973) 259–274.

[7] D.G. Pearson, D. Canil, S.B. Shirey, Mantle samples included in volcanic rocks: xenoliths and diamonds, in: R.W. Carlson (Ed.), Treatise of Geochemistry, The Mantle and Core, vol. 2, Elsevier, Amsterdam, 2003, pp. 171–275.

[8] J. Blichert-Toft, C. Chauvel, F. Albarède, Separation of Hf and Lu for high-precision isotope analysis of rock samples by magnetic sector-multiple collector ICP-MS, Contrib. Mineral. Petrol. 127 (1997) 248–260.

[9] J. Blichert-Toft, On the Lu–Hf isotope geochemistry of silicate rocks, Geostand. Newsl. 25 (2001) 41–56.

[10] J. Blichert-Toft, M. Boyet, P. Tlouk, F. Albarède, ^{147}Sm–^{143}Nd and ^{176}Lu–^{176}Hf in eucrites and the differentiation of the HED parent body, Earth Planet. Sci. Lett. 204 (2002) 167–181.

[11] F.R. Boyd, A pyroxene geotherm, Geochim. Cosmochim. Acta 37 (1973) 2533–2546.

[12] H.N. Pollack, S.J. Hurter, J.R. Johnson, Heat flow from the Earth's interior: analysis of the global data set, Rev. Geophys. 31 (1993) 267–280.

[13] D. Jacob, E. Jagoutz, D. Lowry, D. Mattey, G. Kudrjavtseva, Diamondiferous eclogites from Siberia: remnants of Archean oceanic crust, Geochim. Cosmochim. Acta 58 (1994) 5191–5207.

[14] G.A. Snyder, L.A. Taylor, G. Crozaz, A.N. Halliday, B.L. Beard, V.N. Sobolev, N.V. Sobolev, The origins of Yakutian Eclogite Xenoliths, J. Petrol. 38 (1997) 85–113.

[15] D.G. Pearson, The age of continental roots, Lithos 48 (1999) 171–194.

[16] R.W. Carlson, A.J. Irving, D.J. Schulze, B.C.J. Hearn, Timing of lithospheric mantle modification beneath Wyoming craton, Intern. Kimb. Conf. Proc., 2003, 8 pp., submitted for publication.

[17] S.S. Schmidberger, A. Simonetti, D. Francis, Sr–Nd–Pb isotope systematics of mantle xenoliths from Somerset Island kimberlites: evidence for lithosphere stratification beneath Arctic Canada, Geochim. Cosmochim. Acta 65 (2001) 4243–4255.

[18] S.S. Schmidberger, A. Simonetti, D. Francis, C. Gariépy, Probing Archean lithosphere using the Lu–Hf isotope systematics of peridotite xenoliths from Somerset Island kimberlites, Canada, Earth Planet. Sci. Lett. 197 (2002) 245–259.

[19] P.J. Patchett, Hafnium isotope results from mid-ocean ridges and Kerguelen, Lithos 16 (1983) 47–51.

[20] V.J.M. Salters, A. Zindler, Extreme $^{176}Hf/^{177}Hf$ in the suboceanic mantle, Earth Planet. Sci. Lett. 129 (1995) 13–30.

[21] S.Y. O'Reilly, W.L. Griffin, C.G. Ryan, Residence of trace elements in metasomatized spinel lherzolite xenoliths: a proton-microprobe study, Contrib. Mineral. Petrol. 109 (1991) 98–113.

[22] R.M. Bedini, J.-L. Bodinier, Distribution of incompatible trace elements between the constituents of spinel peridotite xenoliths: ICP MS data from the Earst African rift, Geochim. Cosmochim. Acta 63 (1999) 3883–3900.

[23] M. Günther, E. Jagoutz, Isotopic disequilibria (Sm/Nd, Rb/Sr) between mineral phases of coarse grained, low temperature garnet peridodites from Kimberlite Floors, southern Africa, in: O.H. Leonardos, H.O.A. Meyer (Eds.), Proc. 5th Int. Kimberlite Conf., CPRM, Brazilia, Araxa, Brazil, 1994, pp. 354–365.

[24] R.W. Carlson, A.J. Irving, B.C.J. Hearn, Xenoliths from the Williams kimberlite, Montana: clues to processes of lithosphere formation, modification, and destruction, in: J.J. Gurney, J.L. Gurney, M.D. Pascoe, S.H. Richardson (Eds.), Intern. Kimb. Conf. Proc. vol. 7, Red Roof Design, Cape Town, 1999, pp. 90–98.

[25] N.S.C. Simon, G.I. Irvine, G.R. Davies, D.G. Pearson, R.W. Carlson, The origin of garnet and clinopyroxene in "depleted" Kaapvaal peridotites, Lithos 71 (2003) 289–322.

[26] S. Duchêne, J. Blichert-Toft, B. Luais, P. Télouk, J.-M. Lardeaux, F. Albarède, The Lu–Hf dating of garnets and the ages of the Alpine high-pressure metamorphism, Nature 387 (1997) 586–589.

[27] W.L. Griffin, N.I. Fisher, J.H. Friedman, S.Y. O'Reilly, C.G. Ryan, Cr-pyrope garnets in the lithospheric mantle: 2. Compositional populations and their distribution in time and space, Geochem. Geophys. Geosyst. 3 (2002) DOI:10.1029/2002GC000298.

[28] N. Shimizu, Young geochemical features in cratonic peridotites from Southern Africa and Siberia, in: Y. Fei, C.M. Mysen, B.O. Mysen (Eds.), Mantle Petrology: Field Obser-

vations and High-Pressure Experimentation: A Tribute to Francis R. (Joe) Boyd, Geochem. Soc., Houston, 1999, pp. 47–55.
[29] W.L. Griffin, S.R. Shee, C.G. Ryan, T.T. Win, B.A. Wyatt, Harzburgite to Lherzolite and back again: metasomatic processes in ultramafic xenoliths from the Wesselton kimberlite, Kimberley, South Africa, Contrib. Mineral. Petrol. 134 (1999) 232–250.
[30] D.G. Pearson, G.M. Nowell, The continental lithospheric mantle: characteristics and significance as a mantle reservoir, Philos. Trans. R. Soc., A 360 (2002) 1–28.
[31] J. Ganguly, M. Tirone, R.L. Hervig, Diffusion kinetics of samarium and neodymium in garnet, and a method for determining cooling rates of rocks, Science 281 (1998) 805–807.
[32] J.A. Van Orman, T.L. Grove, N. Shimizu, G.D. Layne, Rare earth element diffusion in a natural pyrope single crystal at 2.8 GPa, Contrib. Mineral. Petrol. 142 (2001) 416–424.
[33] R.W. Carlson, F.R. Boyd, S.B. Shirey, P.E. Janney, T.L. Grove, S.A. Bowring, M.D. Schmitz, J.C. Dann, D.R. Bell, J.J. Gurney, S.H. Richardson, M. Tredoux, A.H. Menzies, D.G. Pearson, R.J. Hart, A.H. Wilson, D. Moser, Continental growth, preservation, and modification in Southern Africa, GSA Today 10 (2000) 1–7.
[34] R.T. Cygan, A.C. Lasaga, Self-diffusion of magnesium in garnet at 750° to 900 °C, Am. J. Sci. 285 (1985) 328–350.
[35] J.R. Farver, R.A. Yund, Silicon diffusion in forsterite aggregates: implications for diffusion creep, Geophys. Res. Lett. 27 (2000) 2337–2340.
[36] T. Hiraga, I.M. Anderson, D.L. Kohlstedt, Chemistry of grain boundaries in mantle rocks, Am. Mineral. 88 (2003) 1015–1019.
[37] S.S. Schmidberger, D. Francis, Nature of the mantle roots beneath the North American craton: mantle xenolith evidence from Somerset Island kimberlites, Lithos 48 (1999) 195–216.
[38] G.J. Irvine, D.G. Pearson, B.A. Kjarsgaard, R.W. Carlson, M.G. Kopylova, G. Dreibus, Evolution of the lithospheric mantle beneath northern Canada: a Re–Os isotope and PGE study of peridotite xenoliths from Somerset Island kimberlites and a comparison to Slave craton lithospheric mantle, Lithos 71 (2003) 461–488.
[39] H.S. Carslaw, J.C. Jaeger, Conduction of Heat in Solids, Oxford Univ. Press, Oxford, 1959, 510 pp.
[40] A. Lachenbruch, Crustal temperature and heat production: implications of the linear heat-flow relation, J. Geophys. Res. 75 (1970) 3291–3300.
[41] S.R. Taylor, S.M. McLennan, The geochemical evolution of the continental crust, Rev. Geophys. 33 (1995) 241–265.
[42] R.L. Rudnick, D.M. Fountain, Nature and composition of the continental crust: a lower crustal perspective, Rev. Geophys. 33 (1995) 267–309.
[43] D.H. Abbott, L. Burgess, J. Longhi, W.H.F. Smith, An empirical thermal history of the Earth's mantle, J. Geophys. Res. 99 (1994) 13835–13850.
[44] D.C. Tozer, The present thermal state of terrestrial planets, Phys. Earth Planet. Inter. 6 (1972) 182–197.
[45] D.L. Turcotte, On the thermal evolution of the Earth, Earth Planet. Sci. Lett. 48 (1980) 53–58.
[46] G. Schubert, D.L. Turcotte, P. Olson, Mantle Convection in the Earth and Planets, Cambridge Univ. Press, Cambridge, 2001, 940 pp.
[47] U.R. Christensen, Thermal evolution models for the Earth, J. Geophys. Res. 90 (1985) 2995–3007.
[48] G.F. Davies, Cooling the core and mantle by plume and plate flows, Geophys. J. Int. 115 (1993) 132–146.
[49] A. Davaille, C. Jaupart, Transient high Rayleigh number thermal convection with large viscosity variation, J. Fluid Mech. 253 (1993) 141–166.
[50] C.P. Conrad, B.H. Hager, The thermal evolution of an Earth with strong subduction zones, Geophys. Res. Lett. 26 (1999) 3041–3044.
[51] J. Korenaga, Energetics of mantle convection and the fate of fossil heat, Geophys. Res. Lett. 30 (2003) DOI: 10.1029/2003GL016982.
[52] R.D. van der Hilst, S. Widiyantoro, E.R. Engdahl, Evidence for deep mantle circulation from global tomography, Nature 386 (1997) 578–584.
[53] C.J. Allègre, The evolution of mantle mixing, Philos. Trans. R. Soc., A 360 (2002) 2411–2431.
[54] F. Albarède, R. van der Hilst, Zoned mantle convection, Philos. Trans. R. Soc., A 360 (2002) 2569–2592.
[55] P.R.A. Wells, Pyroxene thermometry in simple and complex systems, Contrib. Mineral. Petrol. 62 (1977) 129–139.
[56] P. Bertrand, J.-C.C. Mercier, The mutual solubility of coexisting ortho- and clinopyroxene: toward an absolute geothermometer for the natural system? Earth Planet. Sci. Lett., (1986) 109–122.
[57] G.P. Brey, T.P. Köhler, Geothermobarometry in four-phase lherzolites: II. New thermobarometers, J. Petrol. 31 (1990) 1353–1378.
[58] K.G. Nickel, D.H. Green, Empirical geothermobarometry for garnet peridotites and implications for the nature of the lithosphere, kimberlites and diamonds, Earth Planet. Sci. Lett. 73 (1985) 158–170.
[59] D.J. Ellis, D.H. Green, An experimental study of the effect of Ca upon garnet–clinopyroxene Fe–Mg exchange equilibria, Contrib. Mineral. Petrol. 71 (1979) 13–22.
[60] R. Powell, Regression diagnostics and robust regression in geothermometer/geobarometer calibration: the garnet–clinopyroxene geothermometer revisited, J. Metamorph. Geol. 3 (1985) 231–243.
[61] E.J. Krogh, The garnet–clinopyroxene Fe–Mg geothermometer : a reinterpretation of existing experimental data, Contrib. Mineral. Petrol. 99 (1988) 44–48.
[62] S.L. Harley, The solubility of alumina in orthopyroxene coexisting with garnet in $FeO–MgO–Al_2O_3–SiO_2$ and $CaO–FeO–MgO–Al_2O_3–SiO_2$ systems, J. Petrol. 25 (1984) 665–696.